

Final Scientific/Technical Report

Community Petascale Project for Accelerator Science and Simulation

For Grant DOE SC0008491

P.I.: Warren B. Mori

UCLA Departments of Physics and Astronomy and of Electrical Engineering
mori@physics.ucla.edu

Summary:

The UCLA Plasma Simulation Group is a major partner of the “Community Petascale Project for Accelerator Science and Simulation”. This is the final technical report. We include an overall summary, a list of publications, progress for the most recent year, and individual progress reports for each year.

Overall Summary: We have made tremendous progress during the three years. SciDAC funds have contributed to the development of a large number of skeleton codes that illustrate how to write PIC codes with a hierarchy of parallelism. These codes cover 2D and 3D as well as electrostatic solvers (which are used in beam dynamics codes and quasi-static codes) and electromagnetic solvers (which are used in plasma based accelerator codes). We also used these ideas to develop a GPU enabled version of OSIRIS. SciDAC funds were also contributed to the development of strategies to eliminate the Numerical Cerenkov Instability (NCI) which is an issue when carrying laser wakefield accelerator (LWFA) simulations in a boosted frame and when quantifying the emittance and energy spread of self-injected electron beams. This work included the development of a new code called UPIC-EMMA which is an FFT based electromagnetic PIC code and to new hybrid algorithms in OSIRIS. A new hybrid (PIC in r-z and gridless in ϕ) algorithm was implemented into OSIRIS. In this algorithm the fields and current are expanded into azimuthal harmonics and the complex amplitude for each harmonic is calculated separately. The contributions from each harmonic are summed and then used to push the particles. This algorithm permits modeling plasma based acceleration with some 3D effects but with the computational load of an 2D r-z PIC code. We developed a rigorously charge conserving current deposit for this algorithm. Very recently, we made progress in combining the speed up from the quasi-3D algorithm with that from the Lorentz boosted frame. SciDAC funds also contributed to the improvement and speed up of the quasi-static PIC code QuickPIC.

We have also used our suite of PIC codes to make scientific discovery. Highlights include supporting FACET experiments which achieved the milestones of showing high beam loading and energy transfer efficiency from a drive electron beam to a witness electron beam and the discovery of a self-loading regime a for high gradient acceleration

of a positron beam. Both of these experimental milestones were published in *Nature* together with supporting QuickPIC simulation results. Simulation results from QuickPIC were used on the cover of *Nature* in one case. We are also making progress on using highly resolved QuickPIC simulations to show that ion motion may not lead to catastrophic emittance growth for tightly focused electron bunches loaded into nonlinear wakefields. This could mean that fully self-consistent beam loading scenarios are possible. This work remains in progress. OSIRIS simulations were used to discover how 200 MeV electron rings are formed in LWFA experiments, on how to generate electrons that have a series of bunches on nanometer scale, and how to transport electron beams from (into) plasma sections into (from) conventional beam optic sections.

Publications between September 2012 and September 2015:

1. Vieira, J., Martins, J.L., Pathak, V.B., Fonseca, R.A., Mori, W.B., Silva, L.O., "Magnetically assisted self-injection and radiation generation for plasma-based acceleration," *Plasma Physics and Controlled Fusion*, Vol. 54, No., 12, pp. 124044/1-7, Part 1-2 (December 2012).
2. Li, F.Y., Sheng, Z.M., Liu, Y., Meyer-ter-Vehn, J., Mori, W.B., Lu, W., Zhang, J., "Dense attosecond electron sheets from laser wakefields using an up-ramp density transition", *Physical Review Letters*, 110, 135002 (March 2013).
3. Li, F., Hua, J., Xu, X., Zhang, C.J., Yan, L.X., Du, Y.C., Huang, W.H., Chen, H.B., Tang, C.X., Lu, W., Joshi, C., Mori, W.B., Gu, Y.Q., "Generating High-Brightness Electron Beams via Ionization Injection by Transverse Colliding Lasers in a Plasma-Wakefield Accelerator," *Physical Review Letters*, Vol. 111, No. 1, pp. 015003/1-4 (July 2013).
4. An, W., Decyk, V.K., Mori, W.B., Antonson Jr., T.M., "An improved iteration loop for the three dimensional quasi-static particle-in-cell algorithm: QuickPIC," *J. Comp. Phys.*, Vol. 250, pp. 165-177 (October 2013).
5. An, W., Zhou, M., Vafaei-Najafabadi, N., March, K.A., Clayton, C.E., Joshi, C., Mori, W.B., Lu, W., Adii, E., Corde, S., Litos, M., Li, S., Gessner, S., Frederico, J., Hogan, M.J., Walz, D., England, J., Delahaye, J. P., Muggli, P., "Strategies for mitigating the ionization-induced beam head erosion problem in an electron –beam-driven plasma wakefield accelerator", *Physical Review Special Topics Beams and Accelerators* 16, 101301 (October 2013).
6. Xu, X., Yu, P., Martins, S.F., Tsung, F.S., Decyk, V.K., Vieira, J., Fonseca, R.A., Lu, W., Silva, L.O., Mori, W.B., "Numerical instability due to relativistic plasma drift in EM-PIC simulations," *Computer Physics Communication*, vol. 184, No. 11, pp. 2503-2514 (November 2013).
7. Yu, Peicheng, Decyk, Viktor K., An, Weiming, Tsung, Frank S., Mori, Warren B.,

Xu, Xinlu, Lu, Wei, Vieira, Jorge, Fonseca, Ricardo A., Silva, Luis O., "Simulation of Laser wakefield acceleration in the Lorentz boosted frame with UPIC-EMMA," Proceedings of the 2013 North America Particle Accelerator Conference, Pasadena Ca., October 2013.

8. Davidson, A.W., Lu, W., Zheng M., Joshi, C., Silva, L.O., Martins, J., Fonseca, R.A., Mori, W.B., "Self and Ionization-Injection in LFWA for Near-Term Lasers," Proceedings of the 2013 North America Particle Accelerator Conference, Pasadena Ca., October 2013.
9. Fonseca, Ricardo A., Vieira, Jorge, Fiuzza, Frederico, Davidson, Asher, Tsung, Frank S., Mori, Warren B., Silva, Luis O., "Exploiting multi-scale parallelism for large numerical modeling of laser wakefield accelerators," Plasma Physics and Controlled Fusion **55**, 124001 (2013).
10. Litos, M.; Adli, E.; An, W.; Clarke, C. I.; Clayton, C. E.; Corde, S.; Delahaye, J. P.; England, R. J.; Fisher, A. S.; Frederico, J.; Gessner, S.; Green, S. Z.; Hogan, M. J.; Joshi, C.; Lu, W.; Marsh, K. A.; Mori, W. B.; Muggli, P.; Vafaei-Najafabadi, N.; Walz, D.; White, G.; Wu, Z.; Yakimenko, V.; Yocky, G. "High-efficiency acceleration of an electron beam in a plasma wakefield accelerator," Nature **515** 92 (2014).
11. Vieira, J.; Fonseca, R. A.; Mori, W. B.; Silva, L. O. "Ion motion in the wake driven by long particle bunches in plasmas" Physics of Plasmas **21**, 56705 (2014).
12. Shaw, J. L.; Tsung, F. S.; Vafaei-Najafabadi, N.; Marsh, K. A.; Lemos, N.; Mori, W. B.; Joshi, C. "Role of direct laser acceleration in energy gained by electrons in a laser wakefield accelerator with ionization injection" Plasma Physics and Controlled Fusion **56**, 84006 (2014).
13. Viktor K. Decyk and Tajendra V. Singh , "Particle-in-Cell algorithms for emerging computer architectures," Computer Physics Communications 185, 708 (2014).
14. Tzoufras, M.; Tsung, F. S.; Mori, W. B.; Sahai, A. A. "Improving the Self-Guiding of an Ultraintense Laser by Tailoring Its Longitudinal Profile" Physical Review Letters **113**, 245001 (2014).
15. Vieira, J.; Amorim, L. D.; Fang, Y.; Mori, W. B.; Muggli, P.; Silva, L. O. "Self-modulation instability of ultra-relativistic particle bunches with finite rise times" Plasma Physics and Controlled Fusion **56**, 084014 (2014).
16. Ming Zeng; Min Chen; Zheng-Ming Sheng; Mori, W.B.; Jie Zhang. "Self-truncated ionization injection and consequent monoenergetic electron bunches in laser wakefield acceleration" Physics of Plasmas **21**, 30701 (2014)

17. Vafaei-Najafabadi, N., Marsh, K.A., Clayton, C.E., An, W., Mori, W.B., Joshi, C., Lu, W., Adli, E., Corde, S., Litos, M., Li, Gessner, S, Frederico, J., Fisher, A., Wu, Z., Walz, D., England, J., Delahaye, P., Clarke, C., Hogan, M.J., Muggli, P., "Beam loading by a distributed injection electrons in a plasma wakefield accelerator," *Physical Review Letters* **112**, 25001 (2014).
18. Xu, X.L., Hua, J.F., Li, F., Zhang, C.J., Yan, L.X., Du, Y.C., Huang, W.H., Chen, H.B., Tang, C.X., , Lu, W., Yu, P., An, W., Joshi, C., Mori, W.B., "Phase space dynamics of ionization injection in plasma based accelerators", *Physical Review Letters* **112** 035003 (2014).
19. Yu, Peicheng, Xu, Xinlu, Decyk, Viktor K., An, Weiming, Vieira, Jorge, Tsung, Frank S., Fonseca, Ricardo A., Lu, Wei, Silva, Luis O., Mori, Warren B., "Modeling of laser wakefield acceleration in Lorentz boosted frame using an EM-PIC code with a spectral solver", *Journal of Computational Physics*, **266**, 124 (2014).
20. Vieria, J., Muggli, P., Mori, W.B., "Hosing instability suppression in self-modulated plasma wakefields", *Physical Review Letters*, **112** 205001 (2014).
21. Xu, X.L., Wu, Y.P., Zhang, C.J., Li, F., Wan, Y., Hua, J.F., Pai, C-H., Lu, W., Yu, P., Joshi, C., Mori, W.B., " Low emittance electron beam generation from a laser wakefield accelerator using two laser pulses with different wavelengths", *Physical Review Special Topics in Accelerators and Beams*, **17** 61301 (2014).
22. Davidson, A., Tableman, A., An, W., Tsung, Lu, W., Vieira, J., F.S., Fonseca, R., Silva, L.O., Mori, W.B., "Implementation of a hybrid particle code with a PIC description in r-z and a gridless description in f into OSIRIS", *Journal of Computational Physics*, **281**, 1063 (2014).
23. Peicheng Yu, Xinlu Xu, Viktor K. Decyk, Frederico Fiuzza, Jorge Vieira, Frank S. Tsung, Ricardo A. Fonseca, Wei Lu, Luis O. Silva, Warren B. Mori, "Elimination of the numerical Cerenkov instability for spectral EM-PIC codes." *Computer Physics Communications*, **192**, 32 (2015).
24. Decyk, V.K., "Skeleton Particle-in-Cell Codes on Emerging Computer Architectures", *Computing in Science and Engineering*, **17**, 47 (2015).
25. Zeng, M., Chen, M., Yu, L. L., Mori, W. B., Sheng, Z. M., Hidding, B., Jaroszynski, D. A., Zhang, J., "Multichromatic Narrow-Energy-Spread Electron Bunches from Laser-Wakefield Acceleration with Dual-Color Lasers." *Physical Review Letters*, **114**, 084801 (2015).
26. Jain, Neeraj, Palastro, John, Antonson, T. M., Jr., Mori, Warren B., An, Weiming, "Plasma wakefield acceleration studies using the quasi-static code WAKE." *Physics of Plasmas*, **22**, 023103 (2015)

27. Pollock, BB, Tsung, FS, Albert, F, Shaw, JL, Clayton, CE, Davidson, A, Lemos, N, Marsh, KA, Pak, A, Ralph, JE, Mori, WB, Joshi, C, "Formation of Ultrarelativistic Electron Rings from a Laser-Wakefield Accelerator," PHYSICAL REVIEW LETTERS Volume: **115** Issue: 5 Article Number: 055004 Published: JUL 31 2015
28. S. Corde, E. Adli, J. M. Allen, W. An, C. I. Clarke, C. E. Clayton, J. P. Delahaye, J. Frederico, S. Gessner, S. Z. Green, M. J. Hogan, C. Joshi, N. Lipkowitz, M. Litos, W. Lu, K. A. Marsh, W. B. Mori, M. Schmeltz, N. Vafaei-Najafabadi, D. Walz, V. Yakimenko, and G. Yocky "Multi-gigaelectronvolt acceleration of positrons in a self-loaded plasma wakefield" Nature **524** 442 (2015).
29. Peicheng Yu, Xinlu Xu, Adam Tableman, Viktor K. Decyk, Frank S. Tsung, Frederico Fiuzza, Asher Davidson, Jorge Vieira, Ricardo A. Fonseca, Wei Lu, Luis O. Silva, Warren B. Mori, "Mitigation of numerical Cerenkov radiation and instability using a hybrid finite difference-FFT Maxwell solver and a local charge conserving current deposit," submitted to Computer Physics Communications (2015).
30. Xu, X., Wu, Y.P., Zhang, C.J., Li, F., Wan, Y., Hua, J.F., Pai, C.-H., Lu, W., An, W., Yu, P., Mori, W.B., Hogan, M.J., Joshi, C., "Exact phase space matching for staging plasma and traditional accelerator components using longitudinally tailored plasma profiles," submitted to Physical Review Letters
31. Yu, P., Xu, X., Davidson, A., Tableman, A., Dalichaouch, T., Meyers, M.D., Tsung, F.S., Decyk, V.K., Fiuzza, F., Vieira, J., Fonseca, R.A., Lu, W., Silva, L.O., Mori, W.B., "Lorentz boosted frame simulation of Laser wakefield acceleration in quasi-3D geometry," submitted to Journal of Computational Physics.
32. Xu, X., Zhang, C.J., Li, F., Wan, Y., Wu, Y.P., Hua, J.F., Pai, C.-H., Lu, W., An, W., Yu, P., Mori, W.B., Joshi, "Nano-scale electron bunching in laser-triggered ionization injection in plasma accelerators," submitted to Physical Review Letters.
33. Shaw, J.L., Lemos, N., Marsh, K.A., Tsung, F.S., Mori, W.B., Joshi, C., "Estimation of direct laser acceleration in laser wakefield accelerators using particle-in-cell simulations," submitted to Plasma Physics and Controlled Fusion.
34. An, W., Lu, W., Huang, CK, Xu, X, Hogan, M., Joshi, C., Mori, W.B., "Ion motion induced emittance growth of matched electron beams in plasma wakefields" in preparation.

LAST YEAR

ASCR Activities: In the past year, we have continued to implement a variety of fully open source skeleton codes (mini-apps), which are designed to illustrate a variety of parallel algorithms for PIC codes. During the past year, we have extended our 2D skeleton codes 3D. We have implemented electrostatic, electromagnetic, and darwin codes. Darwin (sometimes called magnetostatic or near field electromagnetic) codes include plasma generated electric and magnetic fields generated by plasma currents, but not light waves, and are closely related to quasi-static codes used for plasma accelerators. We have constructed serial, OpenMP, and MPI versions of these 3d codes. Optional Python scripts have also been implemented for all the skeleton codes, which can replace the Fortran or C main codes to enable use of Python capabilities such as graphics, without performance degradation. A paper “Skeleton Particle-in-Cell codes on Emerging Computer Architectures,” was published in Computing in Science and Engineering, vol 17, p. 47 (2015).

HEP Activities:

Software development: During the past year, we have continued to develop algorithms for UPIC-EMMA and OSIRIS that effectively eliminate the NCI thereby enabling Lorentz boosted frame simulations of LWFA. This development includes strategies that permit combining the quasi-3D algorithm with the Lorentz boosted frame capability. We found a better method for recasting the dispersion relation for the NCI which makes it clear that the NCI is a coupling between in the Lorentz boosted frame between modes that are purely EM (transverse) and Langmuir (longitudinal) in the lab frame. There is a coupling between the EM and the infinite set of aliased Langmuir modes. We found that for a spectral solver it was possible to develop strategies to eliminate the three couplings that have the fastest growth rates. These strategies included low pass filters, a reduction in the time step, and a modification of the EM dispersion relation near the coupling. We also found that the same strategies work if the FFT is only done in the drifting direction making the strategies amenable to r-z and quasi-3D geometries. These were implemented in UPIC-EMMA and OSIRIS. For OSIRIS, we also had to develop elimination algorithms that also still used a rigorously conserving charge current deposition. This work will continue.

Scientific Discovery: We have made several scientific discoveries that can be found within the listed publications. Here, we highlight three, two of which were published in *Nature* and the other in *Physical Review Letters*. The articles in *Nature* were milestones in plasma wakefield acceleration (PWFA) research. One milestone is the demonstration of high efficiency, low energy spread acceleration of electrons using a “two bunch” scheme. The second milestone is the demonstration of high energy gain of positrons with low energy spread in a “self-loaded” regime. These experiments were supported by full scale, fully three-dimensional QuickPIC simulations. For the “two-bunch” electron PWFA, the visualization from a QuickPIC simulation results was also chosen as the cover figure for the *Nature* issue of Nov. 6 2014 (shown in Fig. 1). For positron acceleration, the nonlinear plasma wakefield driven by the intense positron bunch is more complicated than those driven by the electron beams. 3D QuickPIC simulations can give us a deeper understanding on the creation and structure of the positron driven plasma wake and on how the positron beam evolves in its own complicated plasma wakefield.

Fig. 2 shows visualizations of the positron driven plasma wake and the positron beam density when it propagates inside the plasma.



Fig. 1: Left: QuickPIC simulation of two-bunch electron-driven PWFA experiment at FACET shown on the *Nature* cover. Middle and right: Visualization of positron beam driven PWFA simulations performed on Blue Waters and appeared in the journal *Nature*. Middle: High density plasma is formed due to the Coulomb field around the positron beam that moves from the bottom to the top. Plasma electrons have wave-like trajectories when they pass by the positron beam; Right: A positron beam is traveling through the plasma from the left to the right. Trajectories of a few positrons oscillating in the charge density wave in the plasma are shown.

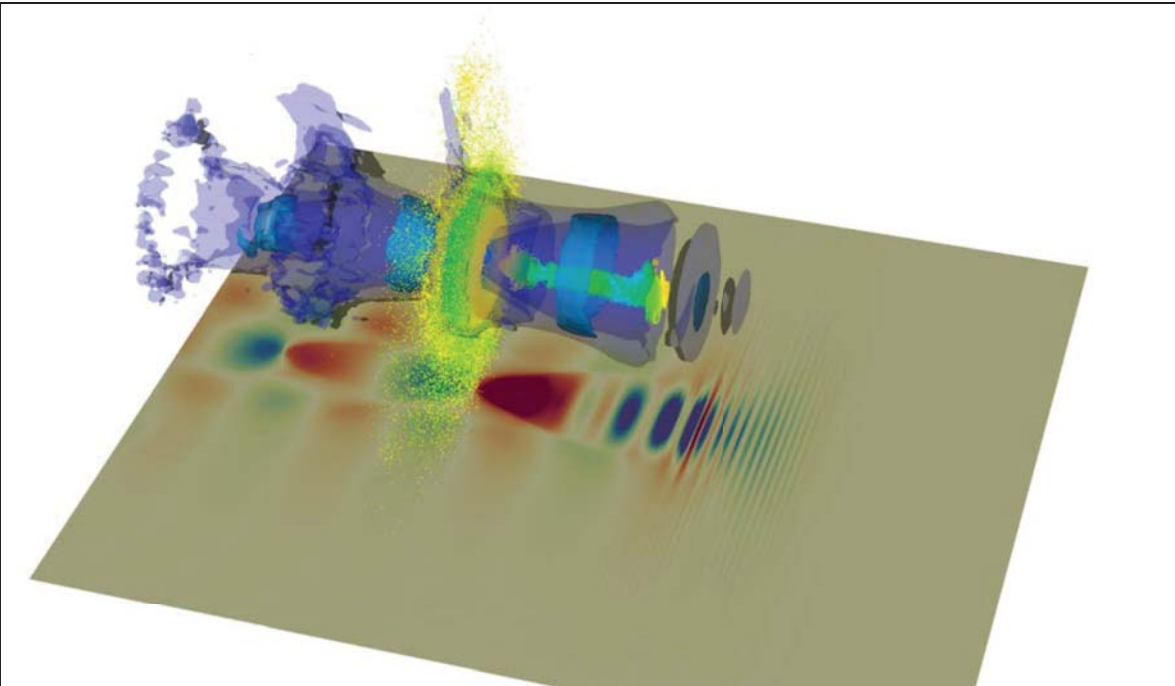


Fig 7: 3D OSIRIS simulation of LWFA experiments on the LLNL CALLISTO laser. OSIRIS simulation showed the formation of a ring structure between the first and the second bucket (which are shown as transparent isosurfaces above). OSIRIS simulations showed good agreements between experiments and simulations (in terms of total charge and the average energy of the ring particles) and gave insights to the formation of the ring structure in experiments.

Furthermore, OSIRIS simulations of recent experiments at the CALLISTO facility gave useful insights on the generation of ultrarelativistic, mono-energetic electron rings from laser wakefield accelerators. Some of these results were reported last year. OSIRIS simulations (shown in Figure 2), showed that the evolution of the laser, both in the transverse direction (due to self-focusing) and the longitudinal direction (due to photo-deceleration) causes the plasma to form toroidal pockets that can trap electrons between the first two buckets and create the annular rings observed in experiments. The process of ring formation depends on the nonlinear evolution of the laser in the blowout regime and can be best studied by first-principle based PIC simulations. This research was published this year in *Physical Review Letters*.

Earlier reports:

YEAR 1

IA. Scaled OSIRIS to the full Blue Waters Sequoia Machines

Late last year OSIRIS was ported to the Blue Waters supercomputer. On Blue Waters we have performed strong scaling studies in both 2D and 3D. In 2D there are 2^{31} ($2^{15} \times 2^{16}$) cells and 256 billion particles and in 3D there are 2^{33} ($2^{11} \times 2^{11} \times 2^{11}$) cells and 256 billion particles. Under these conditions, OSIRIS has shown good scaling for over 256,000 cores. In 2D, the code is >93% efficient without SSE and > 87% efficient with SSE acceleration in 2D, and >78% efficient in 3D with SSE (and >87% without). The results of the scaling study is shown in Figure Scaling.1. In addition, the OSIRIS code achieved a sustained speed of 2.2PFlops on the full Blue Waters platform in 3D using over 10 trillion particles. In the upcoming year we plan to perform 3D simulations of laser plasma interactions using the full Blue Waters machine (>750,000 cpu cores). In addition, OSIRIS was scaled to the full Sequoia Blue/GeneQ computer which has ~1,572,864 cores, <https://www.llnl.gov/news/newsreleases/2013/Mar/NR-13-03-05.html>.

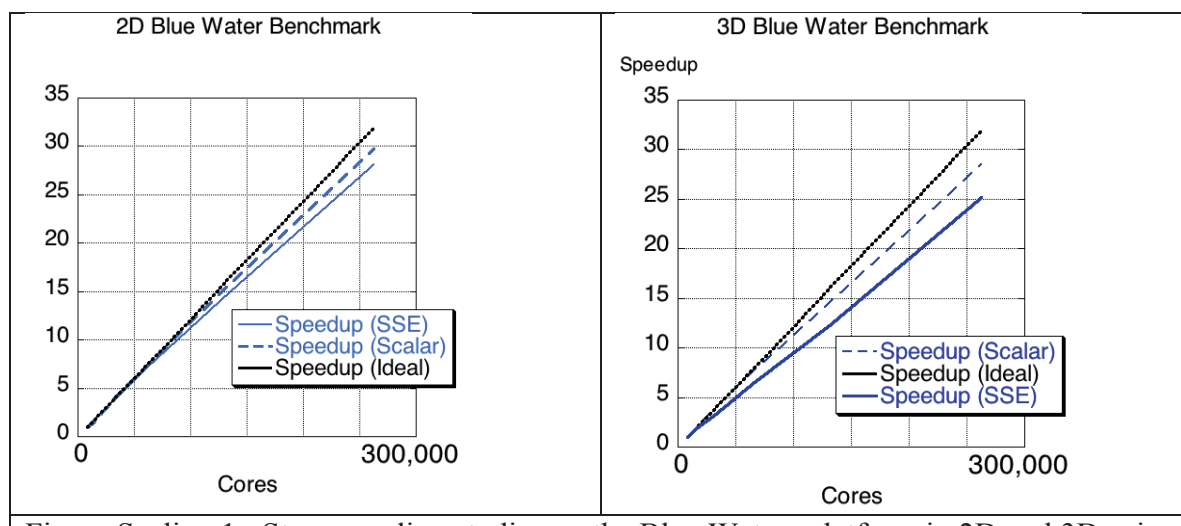


Figure Scaling.1: Strong scaling studies on the Blue Waters platform in 2D and 3D using

256 billion particles. OSIRIS has shown to be >93% efficient in 2D and >87% efficient in 3D

1B. Improved Iteration Loop for QuickPIC:

Recently we implemented a new scheme in QuickPIC for calculating the "time" derivative of the current density by taking the derivative for a finite size particle. This is merged with our new field solver (which was reported previously) that uses a set of gauge invariant equations and requires on one iteration to recover full PIC results for most problems of interest. For a typical nonlinear Plasma Wake Field Accelerator simulation, the new version of QuickPIC runs around 5 times as fast as the old version of QuickPIC when using 4 particles per cell and around 8.5 times as fast when using 25 particles per cell.

In the iteration loop of QuickPIC, we need to calculate $\vec{J}_\perp(\xi + \Delta\xi/2)$ and $\partial\vec{J}_\perp(\xi + \Delta\xi/2)/\partial\xi$. In the old version of QuickPIC, this is done by calculating $\vec{J}_\perp(\xi + \Delta\xi)$ and then taking an average and difference of it with $\vec{J}_\perp(\xi)$. When using domain decomposition, such a scheme requires repartitioning the particles twice within a single pass through the iteration loop. The first particle repartition happens because we need to update the particle position from $\vec{x}(\xi + \Delta\xi/2)$ to $\vec{x}(\xi + \Delta\xi)$ in order to deposit the current density at $\xi + \Delta\xi$. When the particle's position changes, the code needs to move some particles among the processors to make sure they stay in the right partition. The other particle repartition happens at the end of the each pass through the iteration loop. Before we correct the particle position and momentum we need to restore the particle position $\vec{x}(\xi + \Delta\xi/2)$ (the code stores the particle positions at $\xi + \Delta\xi/2$ in the extra memory as well as the velocities at ξ) in order to correct the particle pushing. This requires redistributing the particles among the processors once again.

If we do not change the particle position within the iteration loop, we will not need to repartition the particles during each iteration. This reduces the computer memory needed to store the original particle data and more importantly eliminates the need to repartition the particles during the iteration loop (it only has to be done after the end of the loop).

We accomplish this by depositing $\vec{J}_\perp(\xi + \Delta\xi/2)$ and $\partial\vec{J}_\perp(\xi + \Delta\xi/2)/\partial\xi$ directly at $\xi + \Delta\xi/2$. This method was first introduced in developing a PIC code using the Darwin model [1, 2]. Although different, the quasi-static and Darwin algorithms have many similarities including the ability to use this method. In QuickPIC, to calculate $\vec{J}_\perp(\xi + \Delta\xi/2)$, we need to know the particle momentum at $\xi + \Delta\xi/2$. It can be easily calculated by using $\vec{p}(\xi + \Delta\xi/2) = (\vec{p}(\xi) + \vec{p}(\xi + \Delta\xi))/2$, where $\vec{p}(\xi + \Delta\xi)$ is the corrected particle momentum obtained through the particle push. To deposit $\partial\vec{J}_\perp(\xi + \Delta\xi/2)/\partial\xi$, we use a new method to directly deposit it at $\xi + \Delta\xi/2$ without changing the particle position. This is done by using the following equation for depositing the current density derivative [3],

$$\frac{\partial}{\partial \xi} \vec{J}_\perp = \frac{q}{\text{Vol.}} \left(\sum_i \frac{\frac{\partial}{\partial \xi} \vec{p}_{i\perp}}{1 - \frac{q}{m} \psi} S(\vec{x}_\perp - \vec{x}_{i\perp}) + \sum_i \frac{\vec{p}_{i\perp} \frac{\partial}{\partial \xi} (\frac{q}{m} \psi)}{(1 - \frac{q}{m} \psi)^2} S(\vec{x}_\perp - \vec{x}_{i\perp}) - \nabla_\perp \cdot \sum_i \frac{\vec{p}_{i\perp} \vec{p}_{i\perp}}{(1 - \frac{q}{m} \psi)^2} S(\vec{x}_\perp - \vec{x}_{i\perp}) \right),$$

where $S(\mathbf{x})$ is the particle shape function and $\vec{p}_{i\perp} \vec{p}_{i\perp}$ is a dyadic. This equation shows that $\partial \vec{J}_\perp / \partial \xi$ can be obtained by depositing three different densities evaluated at the particle positions at $\xi + \Delta \xi / 2$. In the first term, $\partial \vec{p}_{i\perp} / \partial \xi$ at $\xi + \Delta \xi / 2$ is the acceleration of the particle. In the second term, $\vec{p}_{i\perp}(\xi + \Delta \xi / 2)$ is calculated from $\vec{p}(\xi + \Delta \xi / 2) = (\vec{p}(\xi) + \vec{p}(\xi + \Delta \xi)) / 2$ and $\partial(q/m \cdot \psi) / \partial \xi$ (note that here ψ is actually $\psi(\vec{x}_{i\perp})$) is calculated from,

$$\frac{\partial}{\partial \xi} \left(\frac{q}{m} \psi \right) = \frac{q}{m} \left(\frac{\partial}{\partial \xi} \psi + \nabla_\perp \psi \cdot \frac{\partial \vec{x}_{i\perp}}{\partial \xi} \right) = \frac{q}{m} \left(E_z + \nabla_\perp \psi \cdot \frac{\vec{p}_{i\perp}}{1 - \frac{q}{m} \psi} \right).$$

Finally, in the third term, after depositing the density dyadic $\vec{p}_{i\perp} \vec{p}_{i\perp}$, we calculate its divergence in Fourier space. None of these three parts requires updating the particle position, which ensures that we can calculate the $\partial \vec{J}_\perp(\xi + \Delta \xi / 2) / \partial \xi$ locally within each processor and no particle relocation is required.

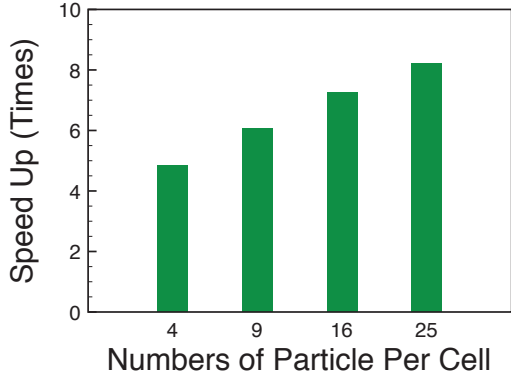


Fig. 2 Total speed up of the new QuickPIC

With this new current derivative deposition scheme and the new field solver based on gauge invariant equations, QuickPIC is significantly faster than before [3]. Figure 2 shows the speed up of the new routine. The test simulation is a nonlinear PWFA case with 512x512x512 cells. Each simulation is run on 64 processors. Both the new version and the old version of QuickPIC use double precision. For this case, the old version required 4 iterations (the field solve and particle push loop is run 5 times) while the new version required only 1 iteration (the loop is run twice). From Fig. 2, we can see that the new code is 5 times faster as the old code when we use 4 particles per cell in the test simulation. And the speedup increases to 8.5 times when there are 25 particles per cell (i.e. more particles on each processor). This additional speed up and the increasing speed up with increasing particle number comes from the reduction in the amount of parallel communication in the new deposition scheme.

Reference

[1]. V. K. Decyk, Darwin Particle-in-Cell Models, The 18th Intl. School/Symposium for Space Simulations, Kauai, Hawaii, USA (2007).

[2]. D. Schriver, et al., Generation of whistler mode emissions in the inner magnetosphere: An event study, J. of Geophysical Res. 115 (2010) A00F17.

[3]. W. An et al., An improved iteration loop for the three dimensional quasi-static particle-in-cell algorithm: Quickpic, (2013), J. Comp. Phys. (submitted).

IIC. Understanding the source of the numerical instability in boosted frame simulations

We investigated the numerical Cherenkov instability observed in the multi-dimension Electromagnetic-Particle-in-cell (EM-PIC) simulations with a plasma drifting with relativistic velocities using both theory and computer simulations [1,2]. We derived the numerical dispersion relation for a cold plasma drifting with a relativistic velocity and find an instability attributed to the coupling between longitudinal like beam modes and electromagnetic modes in the system [see figure 3 (b)-(c)]. The characteristic pattern of the instability in Fourier space for various simulation setups and Maxwell Equation solvers are explored by solving the corresponding numerical dispersion relations. Furthermore, based upon these characteristic patterns we derive an asymptotic expression for the instability growth rate [see figure 3(a)]. We also find there is an optimum time step for reducing the growth rate of this instability when the fields are staggered half cells away from where the current is deposited as arises in finite difference based field solvers. The results do not depend much on the current deposition scheme. The results are compared against simulation results and good agreement is found.

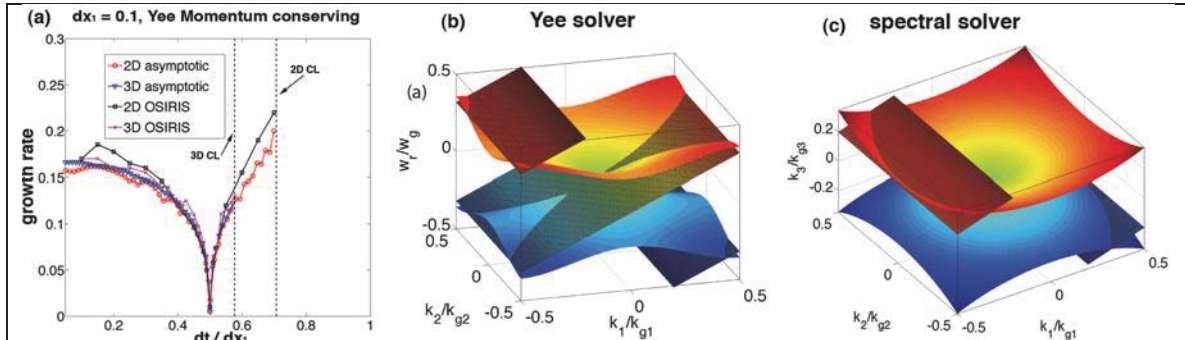


Figure 3: (a) Instability growth rate calculated by the asymptotic expressions; (b) Beam mode intersects with EM modes in Yee solver; and (c) Beam mode intersects with EM modes in the spectral solver.

Using these results as a guide, we developed possible approaches to mitigate the instability. In particular, we examined the use of a spectral solver and showed that such a

solver when combined with a low pass filter with a cutoff value of $|k|$ essentially eliminates the instability.

[1] P. Yu, X. Xu, V. K. Decyk, S. F. Martins, F. S. Tsung, J. Vieira, R. A. Fonseca, W. Lu, L. O. Silva and W. B. Mori, *Modeling of laser wakefield acceleration in the Lorentz boosted frame using OSIRIS and UPIC framework*, in Proceedings of Advanced Accelerator Concept Workshop, Austin TX, 2012

Submitted paper:

[2] Xinlu Xu, Peicheng Yu, Samuel F. Martins, Frank S. Tsung, Viktor K. Decyk, Jorge Vieira, Ricardo A. Fonseca, Wei Lu, Luis O Silva, Warren B. Mori, *Numerical instability due to relativistic plasma drift in EM-PIC simulations*, Computer Physics Communication, in revision.

1D. Development of a multi-dimensional spectral PIC for modeling LWFA in a boosted frame

Based on the study of the numerical Cherenkov instability, we developed a spectral based code for studying laser wakefield accelerator (LWFA) in the Lorentz boosted frame. We developed the UPIC-EMMA codes based on the components of UCLA PIC framework (UPIC) which uses a spectral solver to advance the electromagnetic field in the Fourier space. By using the spectral solver we can constrain the instability to only arise from aliased modes so that the instability occurs for high $|k|$'s in Fourier space. With a low pass (or ring) filter implemented in the spectral solver, the numerical instability can be conveniently mitigated. We verify the feasibility of numerical instability mitigation, as well as the ability to conduct LWFA simulation in the Lorentz boosted frame using UPIC-EMMA. These include the modeling cases where there are no self-trapped electrons, and modeling the self-trapped regime. Detailed comparison among Lorentz boosted frame results and lab frame results obtained from OSIRIS show good agreements between the two cases from a wide range of a_0 (normalized vector potential of the laser). We further verified the accuracy of the boosted frame simulation in UPIC-EMMA by comparing the LWFA stage runs up to 100 GeV.

IE. QuickPIC simulation support of FACET experiments

Recently, we investigated how to mitigate beam head erosion in the field ionized plasma through QuickPIC simulations [1]. The field ionized plasma is produced by E_r field of the drive beam that has a temporally rising charge distribution. The very front of the beam which contains very little charge does not ionize the gas. As a result there are no plasma focusing fields and the front of the beam expands as if it were in vacuum. As the beam begins expand the location of the ionize front slips backwards. In addition, at the location of the ionization front the blowout requires time to occur so this part of the beam does not feel the full focusing force. This leads to different longitudinal slices of the beam to expand at different rates because of beam's finite emittance and the different focusing

forces. Consequently the ionization front continues to recede backward in the beam frame and eventually limits the distance over which the beam can form the wake.

In a pre-formed plasma the phenomenon of beam head erosion is relatively unimportant. This is illustrated in Figure 5(a) where the on axis E_z evolution of the wake produced by an electron beam propagating in a pre-formed plasma is summarized in a "waterfall" plot. In the simulation, FACET parameters were simulated. The electron beam contains $N = 9.6 \times 10^9$ electrons, its r.m.s. spot size is $\sigma_r = 10 \mu\text{m}$, and its r.m.s pulse length is $\sigma_z = 34.1 \mu\text{m}$. The normalized emittance of the beam is $\epsilon_N = 150 \text{ mm mrad}$ and the initial energy of the beam is 22.5 GeV. The initial plasma density is $5 \times 10^{16} \text{ cm}^{-3}$.

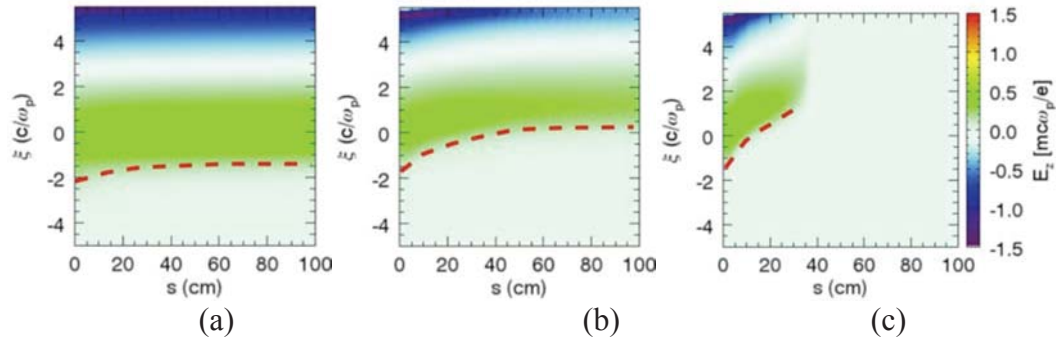


Fig. 5 E_z evolution during the beam propagating in (a) a fully pre-formed plasma;(b) a field ionized Li plasma with the narrow plasma filament;(c) a field ionized Li plasma. The beam is moving downwards and its initial beam center is at $\xi = 0$.

The red dashed lines in the plots show the trajectory of the onset of the wake field (a contour for $E_z = 0.1$). The line has a slope indicating that the ionization front is receding as the beam propagates in the plasma. One can immediately see from Fig. 5(a) there is almost no head erosion in the pre-formed plasma. Unfortunately it is not an easy matter to produce large diameter, uniform density plasmas in the $1.0 \times 10^{16} \sim 5.0 \times 10^{17} \text{ cm}^{-3}$ range. To fully ionize the gas in front of the drive beam, a laser pulse that tunnel or multi-photon ionizes the gas ahead of the drive beam can be used. The drive beam can then excite the plasma wake in this pre-formed plasma. Because the plasma wake has a bubble like shape, the radius of the pre-formed plasma column should be larger than a few times the blow out radius of the wake. This in turn implies that the laser pulse should have enough energy to maintain the intensity above the ionization threshold over the entire volume of the gas that needs to be converted into plasma. This can require rather expensive laser infrastructure particularly if plasma columns that are several meters in length are needed. We therefore explore whether a laser precursor pulse that generates just a narrow filament of plasma in front of the drive beam is sufficient to drastically reduce the beam head erosion. In this case the laser beam ionizes a plasma column that is σ_r (the beam spot size) in radius, just sufficient to produce plasma in the region where E_r is too weak to ionize the neutral gas. Such narrow but long plasma columns can be produced using axicon optics to focus the laser pulse. Figure 6 shows the density plot from a simulation depicting the propagation of the drive beam in a narrow pre-formed plasma column.

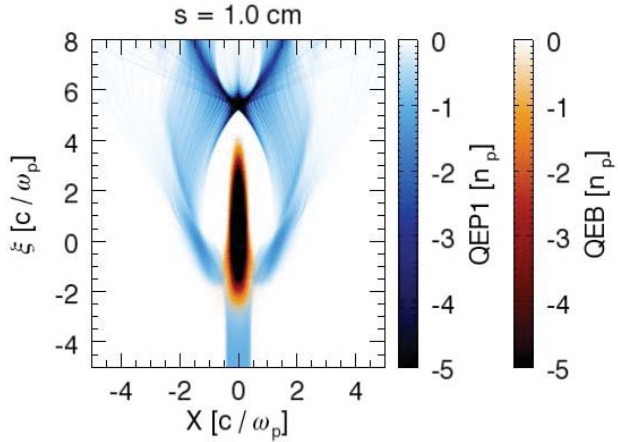


Fig. 6 Density snapshot of the plasma wake with a small preformed plasma column. The plasma electron density has the blue color and the beam density is in brown.

In this simulation, the pre-formed plasma column has a radius of $10 \mu\text{m}$, which is equal to the spot size of the electron beam. Although the plasma filament is not wide enough to include the whole bubble of the wake, it can provide a fully ionized plasma region for the beam head. The Coulomb field of the electron beam subsequently ionizes the neutral gas around the narrow plasma filament and forms the whole wake. Figure 5(b) shows the E_z evolution when the plasma filament exists. As a comparison, we also plot the E_z evolution without the plasma precursor (Fig. 5(c)). From these "waterfall" plots, we can see that when there is no plasma precursor the wake totally disappears after only 30 cm due to beam head erosion. However when the plasma filament is formed ahead of the electron beam, wake goes much further to a distance of greater than 1m. This is because plasma electrons in the filament can immediately be pushed aside by the electron beam thus providing ion focusing force on the front slices of the electron beam keeping it from expanding and thus reducing the head erosion rate. This method can therefore drastically reduce the energy required in the laser pulse by a factor of $(R_b/\sigma_r)^2$, thereby making the laser infrastructure needed more manageable.

Reference

[1]. W. An et al., Strategies for mitigating the beam head erosion problem in a Plasma Wake Field Accelerator, (2013) (prepared for submission).

II. During the first 6 months of the ASCR activities we have:

IIA. Developing PIC algorithms for clusters of GPUs and next generation many cores:

During the past year, we have continued our development of GPU and many-core PIC algorithms. All of our algorithms rely on grouping particles into tiles which contain a small number of grids (typically varying from 2x2 to 16x16 in 2D). Particles are

reordered every time step, so the reordering scheme must be very efficient. Two versions of this underlying approach have been implemented. In the first version, each tile is controlled by a single thread and there are no data collisions, where two threads might attempt to write to the same memory location at the same time. This version is called the collision-free algorithm. In the second version, each tile is controlled by a group of threads, and data collisions are possible. This version is called the collision-resolving algorithm, because it requires efficient mechanisms to resolve data collisions. The collision-free algorithm is best on the NVIDIA GT200 GPUs, while the collision-resolving algorithm works best on the NVIDIA Fermi GPUs. The general structure of both versions is the same, but particle data is transposed in one relative to the other, and the implementation with threads is different.

Crucial to this approach is a fast reordering scheme. The scheme described earlier [Decyk2011] has been improved by storing particles in the outgoing buffers in an ordered way, with all the particles going in a particular direction stored together. The field solver has now also been implemented. Two different 2D real to complex FFTs has been implemented, one based on NVIDIA's underlying FFT library and the other written from scratch. The latter is primarily useful in situations where FFT libraries are not available. On a single GPU, a 2D Electrostatic and a 2-1/2D Electromagnetic code have been written, each with both the collision-free and collision-resolving algorithms. The GPU libraries have been written in Cuda C, but the main code has been written in both C and Fortran.

2D Electrostatic code on M2090 GPU:

Push Time: 0.56 nsec/particle/time step
Deposit Time: 0.25 nsec/particle/time step
Reordering Time: 0.13 nsec/particle/time step
Total Particle Time: 0.94 nsec/particle/time step
(33x total particle speedup compared with 2.67 GHz Intel i7)

2-1/2D Electromagnetic code on M2090 GPU:

Push Time: 0.43 nsec/particle/time step
Deposit Time: 1.24 nsec/particle/time step
Reordering Time: 0.73 nsec/particle/time step
Total Particle Time: 2.40 nsec/particle/time step
(44x total particle speedup compared with 2.67 GHz Intel i7)

The 2D Electrostatic code with the collision-resolving algorithm and parallel FFT has been implemented on multiple GPUs, using CUDA and MPI. The GPU libraries have been written in both Cuda C and Cuda Fortran.

During the code development, an OpenMP version of all the algorithms was implemented as an aide to debugging on the GPU. These OpenMP codes parallelize over tiles. The performance is similar to that achieved with MPI, but the code is compatible with the GPU code (same interface), so that the either the GPU or a traditional processor can be used with the same main code, but with different particle libraries. Additionally, the

particles are ordered, so that interactions which require knowledge of nearby particles, such as collisions, can be easily added.

With the arrival of the Intel PHI, we are extending these OpenMP codes to add an additional level of vectorization using Intel's vector intrinsics. This is being done in collaboration with Ricardo Fonseca from IST. A vector-parallel version of the push and deposit for the 2D electrostatic code using SSE2 instructions has just been implemented, and we are evaluating the results.

All these codes implement what we call skeleton codes: they have all the crucial parts required in a PIC code, but very few diagnostics and initializations required of a production code. As they become stable, our skeleton codes are gradually being made available on the UCLA IDRE web site: <https://idre.ucla.edu/hpc/parallel-plasma-pic-codes>.

References:

Viktor K. Decyk and Tajendra V. Singh , "Adaptable Particle-in-Cell algorithms for graphical processsing units," Computer Physics Communications 182, 641 (2011).

YEAR 2

Summary:

The UCLA Plasma Simulation Group is a major partner of the “Community Petascale Project for Accelerator Science and Simulation”. This is the technical progress report for only the UCLA effort. The UCLA effort is organized into HEP and ASCR activities. We anticipate that we will have \$18,000 to carry over into the final year.

I. During the past year we have made tremendous progress on several fronts in developing new capability in plasma-based accelerator modeling and in using this capability to make scientific discovery (this work is leveraged):

IA. Enhancements to OSIRIS: Implementation of a new hybrid PIC and gridless algorithm for efficient modeling of plasma based acceleration (PI, .1 FTE)

For many plasma physics problems, three-dimensional and kinetic effects are very important. However, such simulations are very computationally intensive. Fortunately, there are a class of problems for which there is nearly azimuthal symmetry and the dominant three-dimensional physics is captured by the inclusion of only a few azimuthal harmonics. Recently, it was proposed by Lifschitz et al. (JCP vol. 228 pp. 1803 2009) to model one such problem, laser wakefield acceleration, by expanding the fields and currents in azimuthal harmonics and truncated the expansion after only the first harmonic. The complex amplitudes of the fundamental and first harmonic for the fields were solved on an r-z grid and a procedure for calculating the complex current amplitudes for each particle based on its motion in Cartesian geometry was presented using a Marder's iterative correction to maintain the validity of Gauss's law. We have implemented this capability into OSIRIS. Our implementation uses a rigorous charge conserving current deposition method to maintain the validity of Gauss's law. We showed that this algorithm is a hybrid method which uses a particles-in-cell description in r-z and a gridless description in the azimuthal angle. We also included the ability to keep an arbitrary number of harmonics and higher order particle shapes. We verified that the charge conservation scheme works and have carried out test cases for laser wakefield acceleration, plasma wakefield acceleration, and beam loading. These tests showed that the important three dimensional physics can be included with speed ups of factors of more than 100 for problems of interest. An example of particle beam hosing is shown in Figure 1. **In the next year(s), we will use this code for physics studies, investigate new boundary conditions, and field solvers. We will also investigate combining the hybrid approach with the ponderomotive guiding center method and the Lorentz boosted frame method for even more dramatic speed ups.**

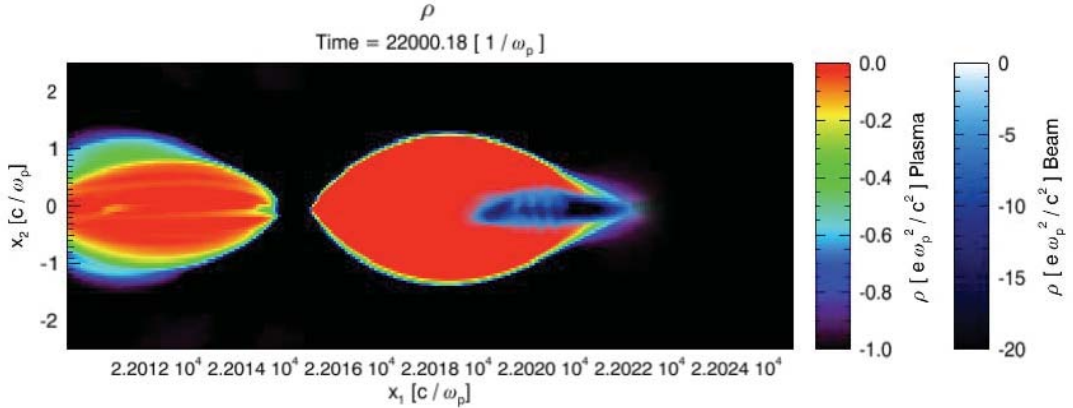


Figure 1: A PWFA simulation using the 2D Hybrid r-z code that shows hosing, i.e., the $m=1$ mode.

1B. Enhancement to LWFA modeling capability: Development of UPIC-EMMA and mitigation of the numerical Cherenkov instability for spectral solvers (PI, .1 of two FTEs)

When modeling plasma based acceleration it can be very advantageous to model the problem in a Lorentz boosted frame where a Lorentz contracted plasma drifts towards a laser (or particle beam). Unfortunately, when a plasma (neutral or single species) drifts with speeds near the speed of light a violent instability called the numerical Cherenkov instability occurs. Recently, we have made much progress in understanding and eliminating this instability. The instability is driven by the coupling between wave particle resonances and electromagnetic waves, including aliasing in time (m) and space (n). We recently published a paper that includes a general dispersion relation for the NCI (the first 3D dispersion relation) that was applicable to finite difference and spectral field solvers. We showed that for finite difference solvers there was an optimum time step to reduce the growth rate while for the spectral solver there was not. We also showed that this optimum time step is the result of a staggered mesh for the electric and magnetic fields. Recently, we have shown that it is easiest to understand the NCI as the coupling between a modes that are purely longitudinal and purely transverse in the rest frame. In a continuous world there is no coupling between these modes in any frame. In the discrete world there is coupling between these modes in the drifting frame. We show that there is a new unstable mode for each aliased mode. We concentrate on the spectral solver and use the dispersion relation to find analytic expressions for each mode. The fast growing mode is due to the first spatial aliased modes and can be eliminated using a low pass filter. The next fastest growing mode is due to the coupling of modes in the fundamental Brillouin zone and they can be eliminated by using a smaller time step. The next fastest growing modes are due to the first time and second spatial aliasing and they can be reduced using higher order particle shapes. We have implemented these strategies into a new fully parallelized, 3D spectral PIC code called UPIC-EMMA (it was rapidly built using the UPIC Framework) to carry out LWFA simulations in a Lorentz boosted frame

with high gamma. Sample results are shown in Figure 2. **In the next year(s), we will enhance boundary conditions, add OpenMP/MPI hybrid parallelization strategy and GPU/Many core capability.**

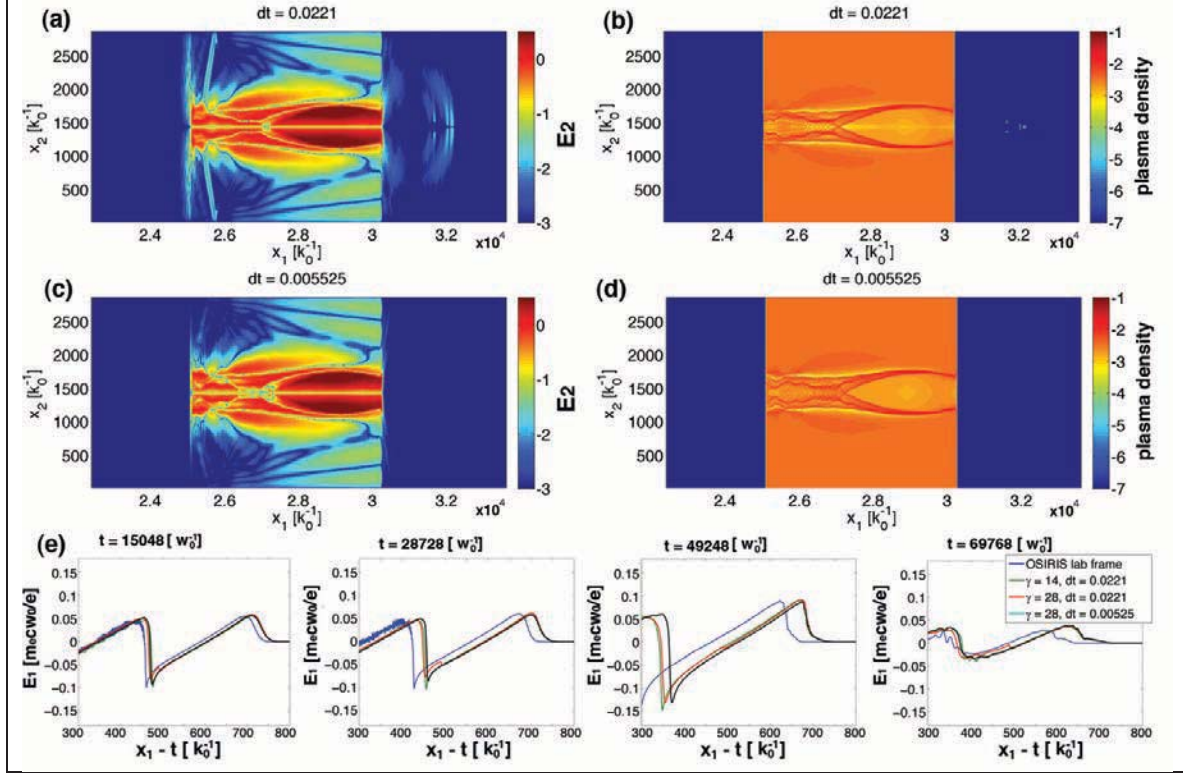


Figure 2: (a) and (b) presents the E_2 and plasma density of the control simulation in [Yu, et. al. J. Comp. Phys. 266, 124 (2014)]; while (c) and (d) are the data from the simulation with a refined recipe to eliminate NCI (in preparation); and (e) the wakefield data transformed back to the lab frame.

1C. Design of a linear collider based on plasma wakefields: Is ion motion really a problem in the blowout regime for linear collider parameters? (.7 post-doc)

One driver for plasma based acceleration (PBA) research is for using this technology to build the next linear collider (LC). One PBA LC concept would be to use PWFA stages to accelerate both electron beam and positron beams to high energies (500 GeV \sim 1 TeV). For the electron arm a very attractive option is to use the nonlinear wakes driven by \sim 20kA electron beams in each stage. These nonlinear wakefields provide ideal properties for accelerating electron beams. However, the focusing forces are so large that the matched spot size of the beam is \sim 100 nm. The high Coulomb field from such tightly focused, high current beams may cause the plasma ions to collapse towards the beam center disrupting the focusing fields. The assumption has been that this would lead to significant emittance growth. However, until now there have been no self-consistent simulations that use cell sizes that resolve the tight spot sizes and ion compression and box sizes encompass the entire volume of the wakefields. We have been moving towards developing the capability to model this phenomenon using the 3D quasi-static PIC code

QuickPIC. In order to self consistently model this problem, a cell size (in transverse direction) on the order of 50 nm is used in the simulation to resolve the beam spot size. This is around 10^4 times less than the typical size of the plasma wake (\sim the skin depth in a $1 \times 10^{17} \text{ cm}^{-3}$ plasma). As a result, a typical simulation for the PWFA linear collider will need a simulation box with at least $8192 \times 8192 \times 2048$ cells. Our preliminary simulations show that the focusing force is significantly enhanced by the ion motion as expected. However, the simulations show that the trailing beam reaches a steady state after around 10 cm of propagation (each stage is \sim 100cm long) and the emittance grows by only a factor of 2, which is much less than expected. We also carried out higher resolution simulations that do not include the driver and the accelerating field (will call these ion only simulations). We have confirmed that the emittance growth from these ion only simulations agree with the fully self-consistent ones for similar resolution. Convergence tests using higher resolution shows even lower emittance growth. In Figure 3 we show results for an ion only simulation with an asymmetric trailing beam. In this case, the trailing beam contains $N = 1 \times 10^{10}$ electrons. The initial rms spot size of the trailing beam in the two transverse directions are $\sigma_x = 464 \text{ nm}$ and $\sigma_y = 73 \text{ nm}$ (the simulation cell size is 12 nm in both the x and y directions). The r.m.s pulse length of the trailing beam is $\sigma_z = 10 \mu\text{m}$. The normalized emittance in the two transverse directions are $\epsilon_{Nx} = 2.0 \text{ mm mrad}$ and $\epsilon_{Ny} = 0.05 \text{ mm mrad}$. The plasma density is $n_p = 1 \times 10^{17} \text{ cm}^{-3}$. In this case, the beam emittance in x direction does not change, and in y directions the emittance just grows by 20%. If these conclusions are born out they could be transformative because beam loading scenarios (simulated earlier with lower transverse resolution) in the nonlinear blowout regime indicate that efficiency of greater than 60 percent can be achieved from the drive beam to the trailing beam while keeping the energy spread less than 1 %. If the emittance can be preserved then there is now a clear research path for the electron arm of a PBA LC. **In the next year(s), we will towards developing the first self-consistent beam loading strategy for a linear collider based on plasma wakefields for either lasers or particle beam drivers.**

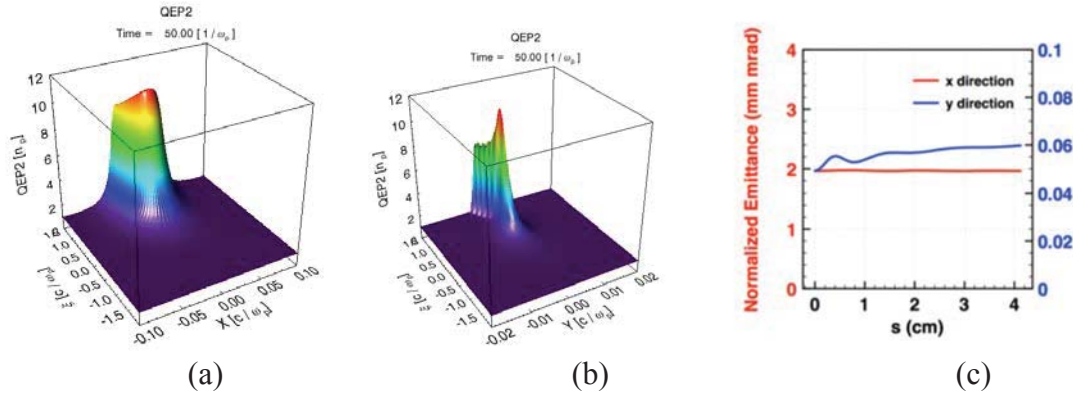


Figure 3: QuickPIC simulation results for a PWFA linear collider case: (a) Snapshot of the plasma ion density (where the trailing beam is located) in the $y=0$ plane; (b) Snapshot of the plasma ion density (where the trailing beam is located) in the $x=0$ plane; (c) The trailing beam's normalized emittance.

1D. Simulation support: Simulation support for FACET (.3 Post-doc and QuickPIC users)

We continue to provide simulation support for the PWFA experiments conducted on FACET at SLAC. The FACET (Facilities for ACcelerator science and Experimental Test beams) provides high energy and high density electron and positron beams with peak current around 20 kA, transverse spot size of 10 μm and an initial energy of 23 GeV. This is a unique program that will mainly focus on the state of art research of PWFA. The Fig. 4 shows QuickPIC simulation results of a recent two-bunch PWFA experiment at FACET, in which a drive bunch is used to excite a large plasma wake and accelerate another trailing bunch following the drive bunch. If the trailing bunch is properly located inside the wake, it can feel a high accelerating gradient (~ 10 GeV/m) while keeping a small energy spread (a few percent) through the high efficient beam loading. The Figure 4 shows a simulation result for parameters near those in the experiment. From Figure 4 (a), we can see that the trailing bunch flattens the longitudinal electric field of the wake, which leads to an almost uniform accelerating field for the trailing bunch itself. As a result, the trailing beam obtains a small energy spread and around 2 GeV energy gain over ~ 30 cm propagation in the plasma. In addition, these results indicate that high energy transfer efficiency may be occurring at FACET.

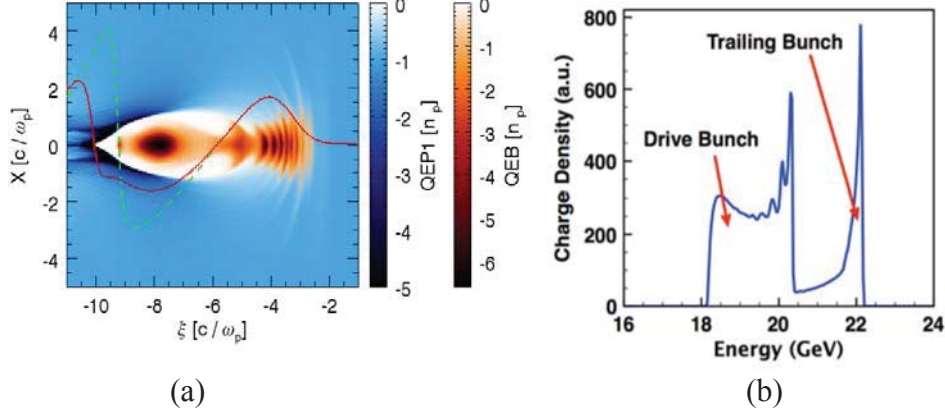


Figure 4: QuickPIC simulation results for a two-bunch PWFA at FACET: (a) The plasma and beam density snapshot in the middle of the simulation. The red line is the on-axis E_z lineout of the plasma wake. The dashed green line is the on-axis E_z lineout of the plasma wake drive by the single drive bunch; (b) The final energy spectra of the drive and trailing bunch.

1E. Simulation support: LWFA simulations of new concepts and experiments (.2 FTE and OSIRIS users)

During the past year, we and collaborators have been using OSIRIS to study transformative concepts (sometimes together with particle beams) to generate ultra bright electron beams and to

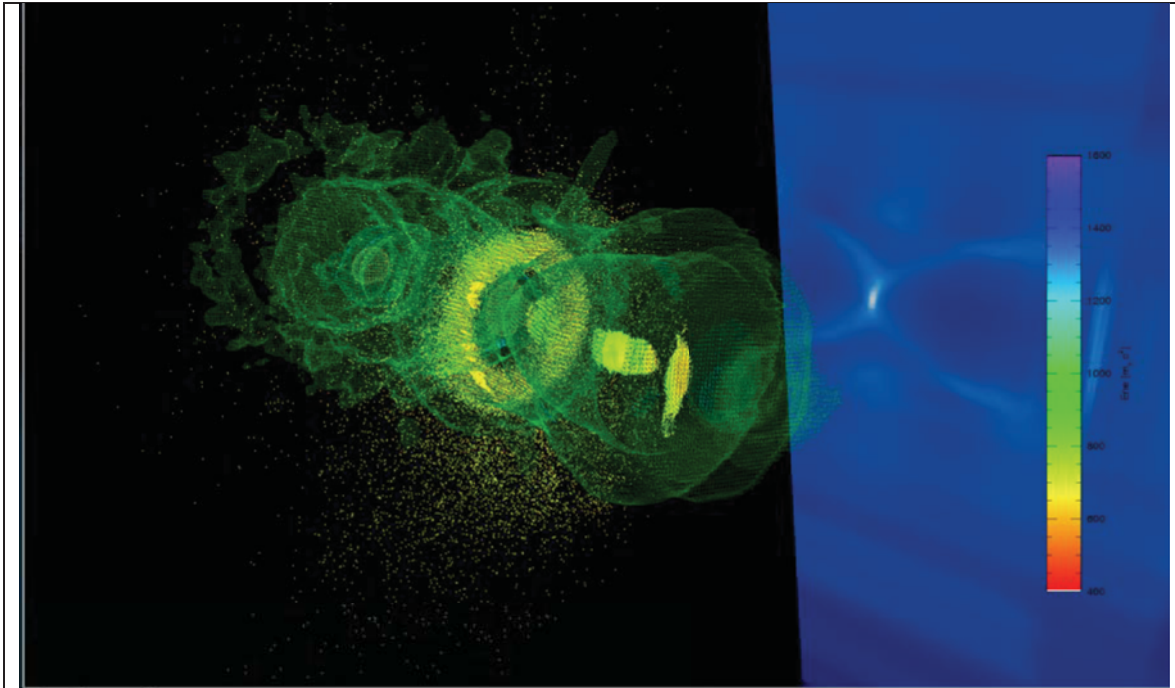


Figure 5: 3D OSIRIS simulation of the Callisto experiment which showed the formation of a monoenergetic electron bunch in the second bucket which is shaped like a ring. The simulation results are being prepared for publication.

study basic physics within LWFA experiments at the Callisto laser at the Jupiter laser facility at LLNL and at UCLA. We published two Physical Review Letters and submitted another paper on how to inject electrons via field ionization into the wake excited by another laser or a particle beam. We have studied using a particle beam or a longer wavelength laser with a large ponderomotive potential but relatively low intensity to excite a wake combined with a shorterwavelength laser with a relatively low ponderomotive potential but a high intensity to trigger the ionization. We found that beams with several pC of charge and sub 10nm emittances can be generated. We have also studied how a ring of electrons can be formed. Experimental evidence from LLNL shows the formation of ring at the ~200-250 MeV range. The formation of the ring was studied in 3D using OSIRIS. The 3D simulations reproduced the ring feature, shown in Figure 5, and it was shown that the formation of the ring comes from a complicated interaction between the laser driver, the trapped electrons in the first bucket, and the background plasma. The simulation and experimental results are being prepared for publication. In addition, in recent LWFA experiments in the quasi-blowout regime, the maximum electron energies measured exceeded theoretical expectations by nearly a factor of 2. We believe that the additional energy gained by the electron beam was due to direct laser acceleration (DLA) being present as an additional acceleration mechanism in the wakefield. Therefore, we have been conducting a series of 3D OSIRIS simulations to explore the role of DLA in LWFA operating in the quasi-linear regime. These simulations are being conducted in a range of experimental parameters that are readily accessible, and they will be used to both confirm experimental data that has already been taken and to guide future experiments. **In the next year(s), we will continue to work to develop new ideas, and to support experiments on generating particle beams with interesting characteristics.**

II. During the past year we have made tremendous progress in developing the UPIC Framework and associated skeleton codes. This work was partially supported by ASCR under the COMPASS project:

IIA. GPU/Many core algorithms and skeleton codes: PIC infrastructure (.2 FTE)

During the past year, the main effort has been to enable our GPU PIC algorithm, developed for a single GPU, to run on multiple GPUS connected with MPI. Details of the single GPU algorithm are available in [Decyk2014]. Both 2D electrostatic and 2-1/2D electromagnetic codes have been implemented, in both Fortran and C, for the Fermi class GPUs. There is a library of procedures written in both Cuda C and Cuda Fortan that can be called from either language. Each MPI node is attached to a single GPU, although there may be multiple GPUs on a single host. For example, our Dawson2 cluster has 3 GPUs per host, so we launch 3 MPI nodes per host. The other cores on the host are not currently used.

There were three important new additions to the single GPU algorithm that were developed. The first addition involved merging the particle reordering with the MPI particle manager. Particles on the GPU are ordered by tile. The GPU reordering scheme first buffers particles going to neighboring tiles. This buffer is ordered by destination. For the multi-GPU version, we extracted those particles leaving at the edges of the tiled domain, and buffered them into a separate MPI buffers, which were then sent to the appropriate GPU. In addition to sending particles, we also had to send a directory (3 words/per tile) which indicated how many of the incoming particles were going in each direction. Programming this with multiple levels of parallelism is tricky, and it has taken us quite a long time to get the bugs out.

The second addition to the single GPU algorithm involved optimizing the all-to-all transpose needed by the FFT. In the single GPU version, the transpose is done entirely by Cuda kernels on the GPU. In the distributed version, a local transpose is first done on the GPU, copied to the host, sent via MPI to all the other GPUs, then copied by the

remote hosts to their GPU. To optimize this transpose, the local transpose on the GPU was unchanged, since it is much faster than the data movement involving the host. To improve the performance, we used a triple buffering scheme with asynchronous sends and receives. Thus the copy from the GPU to the host for one segment was overlapped with an MPI send/receive of a different segment, and with a copy from the host to the GPU of a third segment.

The third addition to the single GPU algorithm was a procedure to assign an MPI node to a GPU device id. This was needed for the case with multiple GPUs on a single host to make sure that each MPI node was assigned a different GPU, and was done by making use of the MPI_GET_PROCESSOR_NAME procedure. Each MPI node sent a message containing its name to every other node. If the incoming name matched its own, the node

would then add that processor id to a list. The list was then locally sorted in increasing processor order, and each processor would then find the index in that list that contained its own processor id. That index then gave the GPU device id that MPI node would assign itself to.

As the codes are fully debugged and documented, they are posted on our public web site at: <https://idre.ucla.edu/hpc/parallel-plasma-pic-codes>. Currently, there are example codes for a single GPU as well as OpenMP and OpenMP/MPI codes which use the same algorithms as the GPU, but are substantially easier to understand. **In the next year(s), we will incorporate these algorithms into production codes, improve the strong scaling of the algorithms, and begin to extend the algorithms to 3D codes as well. The goal is to have an algorithm that can work on general many core architectures, including GPUs and Phis.**

Publications between March 2013 and March 2014:

1. Li, F.Y., Sheng, Z.M., Liu, Y., Meyer-ter-Vehn, J., Mori, W.B., Lu, W., Zhang, J., “Dense attosecond electron sheets from laser wakefields using an up-ramp density transition”, Physical Review Letters, 110, 135002 (March 2013).
2. Li, F., Hua, J., Xu, X., Zhang, C.J., Yan, L.X., Du, Y.C., Huang, W.H., Chen, H.B., Tang, C.X., Lu, W., Joshi, C., Mori, W.B., Gu, Y.Q., “Generating High-Brightness Electron Beams via Ionization Injection by Transverse Colliding Lasers in a Plasma-Wakefield Accelerator,” Physical Review Letters, Vol. 111, No. 1, pp. 015003/1-4 (July 2013).
3. An, W., Decyk, V.K., Mori, W.B., Antonson Jr., T.M., “An improved iteration loop for the three dimensional quasi-static particle-in-cell algorithm: QuickPIC,” J. Comp. Phys., Vol. 250, pp. 165-177 (October 2013).
4. An, W., Zhou, M., Vafaei-Najafabadi, N., March, K.A., Clayton, C.E., Joshi, C., Mori, W.B., Lu, W., Adii, E., Corde, S., Litos, M., Li, S., Gessner, S., Frederico, J., Hogan, M.J., Walz, D., England, J., Delahaye, J. P., Muggli, P., “Strategies for mitigating the ionization-induced beam head erosion problem in an electron – beam-driven plasma wakefield accelerator”, Physical Review Special Topics Beams and Accelerators 16, 101301 (October 2013).
5. Xu, X., Yu, P., Martins, S.F., Tsung, F.S., Decyk, V.K., Vieira, J., Fonseca, R.A., Lu, W., Silva, L.O., Mori, W.B., “Numerical instability due to relativistic plasma drift in EM-PIC simulations,” Computer Physics Communication, vol. 184, No. 11, pp. 2503-2514 (November 2013).

6. Yu, Peicheng, Decyk, Viktor K., An, Weiming, Tsung, Frank S., Mori, Warren B., Xu, Xinlu, Lu, Wei, Vieira, Jorge, Fonseca, Ricardo A., Silva, Luis O., "Simulation of Laser wakefield acceleration in the Lorentz boosted frame with UPIC-EMMA," Proceedings of the 2013 North America Particle Accelerator Conference, Pasadena Ca., October 2013.
7. Davidson, A.W., Lu, W., Zheng M., Joshi, C., Silva, L.O., Martins, J., Fonseca, R.A., Mori, W.B., " Self and Ionization-Injection in LFWA for Near-Term Lasers," Proceedings of the 2013 North America Particle Accelerator Conference, Pasadena Ca., October 2013.
8. Fonseca, Ricardo A., Vieira, Jorge, Fiuzza, Frederico, Davidson, Asher, Tsung, Frank S., Mori, Warren B., Silva, Luis O., "Exploiting multi-scale parallelism for large numerical modeling of laser wakefield accelerators," *Plasma Phys. Control. Fusion* 55 (2013) 124011.
9. Vafaei-Najafabadi, N., Marsh, K.A., Clayton, C.E., An, W., Mori, W.B., Joshi, C., Lu, W., Adli, E., Corde, S., Litos, M., Li, Gessner, S, Frederico, J., Fisher, A., Wu, Z., Walz, D., England, J., Delahaye, P., Clarke, C., Hogan, M.J., Muggli, P., "Beam loading by a distributed injection electrons in a plasma wakefield accelerator," submitted to *Physical Review Letters*.
10. Xu, X.L., Hua, J.F., Li, F., Zhang, C.J., Yan, L.X., Du, Y.C., Huang, W.H., Chen, H.B., Tang, C.X., Lu, W., Yu, P., An, W., Joshi, C., Mori, W.B., "Phase space dynamics of ionization injection in plasma based accelerators", *Physical Review Letters* vol. 112 035003:1-4 January 23 2014.
11. Viktor K. Decyk and Tajendra V. Singh , "Particle-in-Cell algorithms for emerging computer architectures," *Computer Physics Communications* 185, 708 (2014).
12. Yu, Peicheng, Xu, Xinlu, Decyk, Viktor K., An, Weiming, Vieira, Jorge, Tsung, Frank S., Fonseca, Ricardo A., Lu, Wei, Silva, Luis O., Mori, Warren B., "Modeling of laser wakefield acceleration in Lorentz boosted frame using an EM-PIC code with a spectral solver", to appear in *Journal of Computational Physics*.
13. Vieria, J., Muggli, P., Mori, W.B., "Hosing instability suppression in self-modulated plasma wakefields", to appear in *Physical Review Letters*.
14. Xu, X. L., Wu, Y. P., Zhang, C. J., Li, F., Wan, Y., Hua, J. F., Pai, C.-H., Lu, W., Yu, P., Joshi, C., Mori, W. B., "Low emittance electron beam generation from a laser wakefield accelerator using two laser pulses with different wavelengths", submitted to *Physical Review Special Topics Accelerators and Beams*.

15. Davidson, A., Tsung, F.S., Fonseca, R., Mori, W.B., “Implementation of a hybrid particle code with a PIC description in r-z and a gridless description in ϕ into OSIRIS”, submitted to Journal of Computational Physics.
16. Yu, Peicheng, Xu, Xinlu, Decyk, Viktor K., An, Weiming, Vieira, Jorge, Tsung, Frank S., Fonseca, Ricardo A., Lu, Wei, Silva, Luis O., Mori, Warren B., “Elimination of the Numerical Cerenkov related instabilities using spectral EM-PIC codes”, in preparation.